Improvement in estimation of soil water deficit by integrating airborne imagery data into a soil water balance model

Huihui Zhang[1], Ming Han[1,2], José L. Chávez[2], Yubin Lan[3*]

(1. *Water Management and Systems Research Unit, USDA-ARS, 2150 Centre Avenue, Bldg. D., Fort Collins, CO, 80526, USA*;
2. *Department of Civil and Environmental Engineering, Colorado State University, Campus Delivery 1372, Fort Collins, CO, 80523, USA*;
3. *College of Engineering, South China Agricultural University/Engineering Research Center for Agricultural Aviation Application (ERCAAA), Guangzhou 510642, China*)

Abstract: In this study, an approach that integrates airborne imagery data as inputs was used to improve the estimation of soil water deficit (SWD) for maize and sunflower grown under full and deficit irrigation treatments. The proposed model was applied to optimize the maximum total available soil water (TAWr) by minimizing the difference between a water stress coefficient k_s and crop water stress index (1-CWSI). The optimal value of maximum TAWr was then used to calibrate a soil water balance model which in turn updated the estimation of soil water deficit. The estimates of SWD in the soil profile of both irrigated maize and sunflower fields were evaluated with the crop root zone SWD derived from neutron probe measurements and the FAO-56 SWD procedure. The results indicated a good agreement between the estimated SWD from the proposed approach and measured SWD for both maize and sunflower. The statistical analyses indicated that the maximum TAWr estimated from CWSI significantly improved the estimates of SWD, which reduced the mean absolute error (MAE) and root mean square error (RMSE) by 40% and 44% for maize and 22% for sunflower, compared with the FAO-56 model. The proposed procedure works better for crops under deficit irrigation condition. With the availability of higher spatial and temporal resolution airborne imagery during the growing season, the optimization procedure can be further improved.

Keywords: soil water deficit, soil water balance model, airborne imagery, total available water, CWSI, deficit irrigation
DOI: 10.3965/j.ijabe.20171003.3081

Citation: Zhang H H, Han M, Chávez J L, Lan Y B. Improvement in estimation of soil water deficit by integrating airborne imagery data into a soil water balance model. Int J Agric & Biol Eng, 2017; 10(3): 37–46.

1 Introduction

In arid and semi-arid regions of the world, water scarcity is one of the most important challenges for agricultural water management. Crop production heavily depends on adequate soil moisture storage in the root zone. Thus, accurate knowledge related to root zone soil water deficit is required for irrigation management in order to maximize water use efficiency under limited water supplies.

Soil water balance models have been used for irrigation management. Over the last few decades, the dual crop coefficient approach described in FAO-56 manual[1] has been widely accepted as a tool for irrigation scheduling. The generally called "Two-step" methodology distinguishes crop transpiration (T) and soil evaporation (E) using two key variables, basal crop coefficient (k_{cb}) and reference (e.g., grass) evapotranspiration (ET_o). The k_{cb} is defined as the ratio between crop potential transpiration and ET_o and used to

Received date: 2017-04-18 **Accepted date:** 2017-05-20
Biographies: Huihui Zhang, PhD, Research Scientist, research interests: agricultural water management, remote sensing for mapping ET and other related areas, Email: Huihui.Zhang@ars.usda.gov; **Ming Han**, PhD, Postdoctor, research interests: agricultural remote sensing and hydrology modeling, Email: dustming@gmail.com; **José L. Chávez**, PhD, Associate Professor, Irrigation Specialist, research interests: irrigation water management, crop/vegetation water consumptive use (evapotranspiration, ET) determination and modeling, Email: jlchavez@rams.colostate.edu.
***Corresponding author: Yubin Lan**, PhD, Professor, research interest: agricultural aviation application. International Laboratory of Agricultural Aviation Pesticide Spraying Technology, South China Agricultural University, Guangzhou 510642, China. Tel: +86-20-85281421, Email: ylan@scau.edu.cn.

determine crop potential transpiration under well-watered conditions. For crop under water limited conditions, actual transpiration will be limited by soil water supply[2]. In this situation, the water stress coefficient (k_s) will multiply k_{cb} to count for the influence of water stress on crop transpiration. Total available water at root zone (TAWr)[3-5] is the important parameter to determine k_s, and deep percolation. Furthermore, TAWr is influenced by crop variety, root depth, and soil properties[3].

A few studies have been conducted to improve the estimation of soil water content. Sánchez et al.[6] introduced satellite-based NDVI (normalized difference vegetation index) for the calculation of k_{cb} in FAO-56 water balance model for spatially distributed simulation of soil moisture at watershed scale. Neale et al.[7] proposed a hybrid model that corrects ET estimated by the two-energy balance model (TSEB) using the ET provided by a reflectance-based crop coefficient model. The corrected ET then was used in a soil water balance model to estimate soil water content for a cotton crop. More recently, Campos et al.[8] have combined actual ET measurements with a soil water balance model to estimate total available soil water in vineyards. However, in-situ evapotranspiration measurement is not always available.

Canopy temperature increases in response to water stress and water shortage in root zone. It has been used widely as an indicator of crop water status. Canopy temperature can be easily acquired using infrared thermometers or infrared thermal cameras. Canopy temperature measured by thermal cameras has been used to directly estimate soil water deficit[9]. Crop water stress index (CWSI), calculated from canopy temperature, has also been used successfully to determine crop water stress[10-12]. The stress coefficient k_s can be estimated from CWSI as 1-*CWSI*. CWSI is mathematically defined in Equation (1)[13,14]. Where the upper term in the equation $(T_c-T_a)_u$ represents the upper limit or boundary while in the denominator of the equation $(T_c-T_a)_l$ represents the lower boundary. In the equation, T_c-T_a stands for temperature difference between canopy and air.

$$CWSI_i = \frac{(T_c - T_a)_i - (T_c - T_a)_l}{(T_c - T_a)_u - (T_c - T_a)_l} \quad (1)$$

where, $(T_c - T_a)_i$ is the difference between canopy temperature (T_c, °C) and air temperature (T_a, °C) for day *i*. $(T_c-T_a)_u$ and $(T_c-T_a)_l$ represent non-transpiring and fully transpiring conditions, respectively.

When a crop is under full water condition, CWSI value is close to 0; while for a crop under severe water stress condition, CWSI value is close to 1. $(T_c - T_a)_u$ and $(T_c - T_a)_l$ can be estimated as linear functions of atmospheric vapor pressure deficit (VPD) and vapor pressure gradient (VPG), respectively:

$$(T_c - T_a)_l = a \cdot VPD + b \quad (2)$$

$$(T_c - T_a)_u = a \cdot VPG + b \quad (3)$$

where, a and b are the slope and intercept of linear equations, respectively. These two linear relationships are called water stress baselines. In this study, we used the water stress baselines that have been developed for the study area by DeJonge et al.[15] and Taghvaeian et al.[16]

Thus, the goal of this study was to investigate the capability of the crop water stress index, calculated from airborne thermal imagery, to optimize the estimation of total available water in the crop root zone. The proposed approach used data assimilation techniques to update soil water deficit values using an optimal maximum total available water by minimizing the difference between k_s calculated by a soil water balance method[1] and 1-CWSI.

2 Materials and methods

2.1 FAO-56 soil water balance model

According to Allen et al.[17], the root zone soil water balance, at daily time steps, is given by the Equation (4) below.

$$Dr_i = Dr_{i-1} + T_i + E_i + DP_i - (P_i - RO_i) - I_i - CR_i \quad (4)$$

where, Dr_i is the root zone soil water deficit on day *I*; Dr_{i-1} is soil water deficit on day $i-1$; T_i is actual plant transpiration on day *I*; E_i is soil evaporation on day *I*; P_i and I_i are gross precipitation and irrigation, respectively, on day *I*; DP_i is deep water percolation from the root zone on day *I*; RO_i is the runoff from soil surface on day *I*; and CR_i is the capillarity rise from the ground water. The units of the above components are in mm.

In this study, we assumed there was no surface runoff (RO_i) in the field (low slope and moderately high soil

infiltration), and the capillarity rise (CR_i) from the 6 m deep water table was assumed to be negligible. The maximum maize root zone depth observed in this field was around 1.05 m[18]. The Dr_i is determined by the FAO-56 approach[17], which is limited by the total plant available water in the root zone. The minimum value of Dr_i is zero, when soil water content is at field capacity.

According to Allen et al.[17], actual transpiration (T_i) and actual soil evaporation (E_i) in Equation (4) are determined by the dual coefficient method:

$$T_i = k_{s,i} \times k_{cb,i} \times ET_{0,i} \quad (5)$$

$$E_{s,i} = k_{e,i} \times ET_{0,i} \quad (6)$$

where, $k_{s,i}$ is the water stress coefficient, which ranges from 0 to 1 and decreases crop transpiration based on soil water availability; $k_{cb,i}$ is the basal crop coefficient, which is the ratio of crop potential transpiration to reference crop evapotranspiration; $ET_{0,i}$ is the reference crop evapotranspiration (grass based) on day I; and $k_{e,i}$ is soil water evaporation coefficient on day i.

2.1.1 Water stress coefficient k_s

The water stress coefficient k_s is affected by $TAWr$, D_r, and potential transpiration rate. Colaizzi et al.[19] found that k_s determined by the approach suggested by Jensen et al.[20] had a better correlation with CWSI than the k_s from the FAO-56 approach[17]. Thus, in this study, the k_s was defined as[19,20]:

$$k_{s,i} = \frac{\ln[(1 - fDEP_{i-1}) \times 100 + 1]}{\ln(101)} \quad (7)$$

where, the $fDEP_{i-1}$ is the ratio of root zone soil water deficit on day $i-1$ (Dr_{i-1}) and root zone total available water on day i ($TAWr_i$).

2.1.2 Total available soil water at root zone (TAWr)

TAWr is affected by soil texture and rooting depth[17]. In this study, we directly determine the TAWr development with four parameters: t_1, t_x, $TAW_{\min}$, and $TAW_{\max}$ in Equation (8).

$$\begin{cases} TAWr_i = TAW_{\min}, \text{When } t_i < t_1 \\ TAWr_i = TAW_{\min} + (TAW_{\max} - TAW_{\min}) \dfrac{t_i - t_1}{t_x - t_1}, \\ TAWr_i = TAW_{\max}, \text{When } t_i > t_x \end{cases}$$

$$\text{When } t_1 < t_i < t_x \quad (8)$$

where, t_1 is the day after planting, before which the root did not begin to develop; $TAW_{\min}$ is the total available water in root zone in this period (from planting to t_1). The t_x is the day after planting when crop root reach its maximum depth, and the $TAW_{\max}$ is the maximum root zone total available water at that time (after t_x).

2.2 Inversion procedure for TAWr estimation

In the above soil water balance model, the unknown parameters are t_1, t_x, $TAW_{\min}$, $TAW_{\max}$ in Equation (8). The parameter t_1, t_x, $TAW_{\min}$ were obtained from a previous water balance study at the same field, which were 7, 68 and 18.25, respectively[21]. The soil water balance model estimates the daily D_r, and then the D_r can be used to estimate the daily water stress coefficient k_s by a given $TAW_{\max}$. Alternatively, k_s can be calculated by (1–$CWSI$). Therefore, we propose an optimized procedure to estimate $TAW_{\max}$ by minimizing the difference between the k_s calculated from a soil water balance model and k_s from canopy temperature measurements denoted as k_{s_CWSI} (Figure 1). In the optimization process, the Nash coefficient in Equation (9) was used to evaluate the difference between k_s and k_{s_CWSI}. The optimization procedure was completed by using a multi-objective optimization package (mco) in the statistical program R[22]. The objective function was defined as follows[22]:

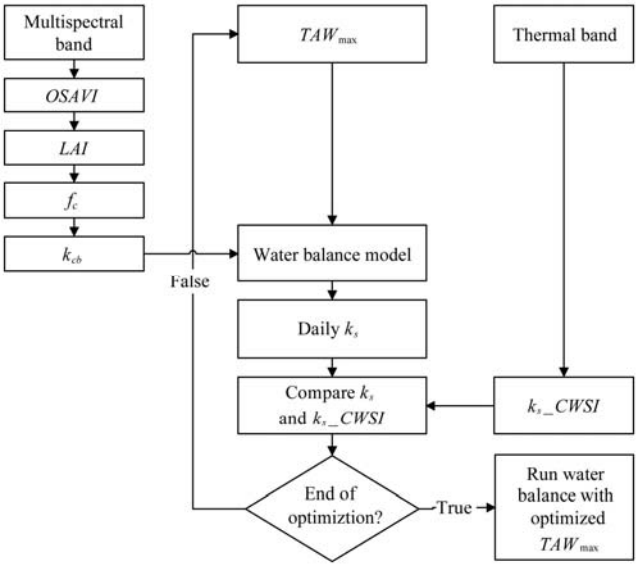

Figure 1 Flowchart of optimized $TAW_{\max}$ with CWSI

Minimize:

$$Nash = \frac{\sum_{i=1}^{n} (k_{s,i} - k_s\_CWSI_i^n)^2}{\sum_{i=1}^{n} (k_s\_CWSI_i - \bar{k}_s\_CWSI)^2} \quad (9)$$

where, n is the total number of observation; $\overline{k}_{s,i}$ and k_{s_CWSIi} are the daily mean values of water stress from the soil water balance model and CWSI, respectively.

2.3 Experimental data

2.3.1 Study site

An experiment was conducted on maize (*Zea mays* L.) and sunflower (*Helianthus annuus L.*) fields during the summer of 2015 at the USDA-ARS Limited Irrigation Research Farm (LIRF), in Greeley, Colorado, USA (40°26'57"N, 104°38'12"W, elevation 1427 m, Figure 2). The alluvial soils of the study field are predominantly sandy and fine sandy loam of Olney and Otero series. The maize and sunflower were planted on June 1 (DOY 152) and June 16 (DOY 167) in 2015, respectively. The plant density was 80 000 seeds/hm^2 for maize and 67 200 seeds/hm^2 for sunflower. During the growing season, twelve irrigation treatments, with varying levels of regulated deficit irrigation (RDI) (Table 1, Column 1), were arranged in a randomized block design with four replications (Figure 2). The deficit irrigation was applied during the late vegetative growth stage and/or the maturation growth stage, which are V7-V21 and R3-R6 in maize; and V8-R2 and R6-R9 in sunflower. Each treatment targeted a percent of maximum non-stressed crop ET during late vegetative and maturation growth stages, respectively. Each treatment plot was 9 m wide by 43 m long with 12 rows at 0.76 m spacing. Sum of actual net irrigation amounts and precipitation for each treatment by growth stage are shown in Table 1. During the growing season in 2015, water was applied using 16 mm internal diameter drip irrigation tubing, which was placed next to each row of maize. Fertilizers were applied same amount to avoid nutrient deficiencies on all the treatments[15]. Meteorological data were acquired by the on-site Colorado Agricultural Meteorological Network GLY04 weather station (CoAgMet, http://ccc.atmos.colostate.edu/ ~ coagmet/). The measurements included hourly air temperature, relative humidity, incoming shortwave solar radiation, horizontal wind speed at 2 m above a grass reference surface, and daily precipitation.

Table 1 Total net irrigation and precipitation (mm) for each treatment in maize and sunflower for different growth stages

Treatment	Maize			Sunflower		
	Veg 6/2-8/3	Rep 8/4-8/24	Mat 8/25-10/10	Veg 6/17- 8/12	Rep 8/13-9/2	Mat 9/3-10/10
100/100	166	116	199	186	73	161
100/50	166	90	33	185	47	25
80/80	126	108	146	133	57	132
80/65	126	98	87	134	58	69
80/40	40	111	149	53	62	132
65/80	126	110	0	135	58	1
65/65	84	111	159	98	63	132
65/50	84	112	69	98	57	69
65/40	85	112	24	100	62	25
50/50	85	114	0	97	63	1
40/40	54	113	24	58	62	25
40/80	40	113	0	52	63	1
Precipitation	76	23	9	30	20	9

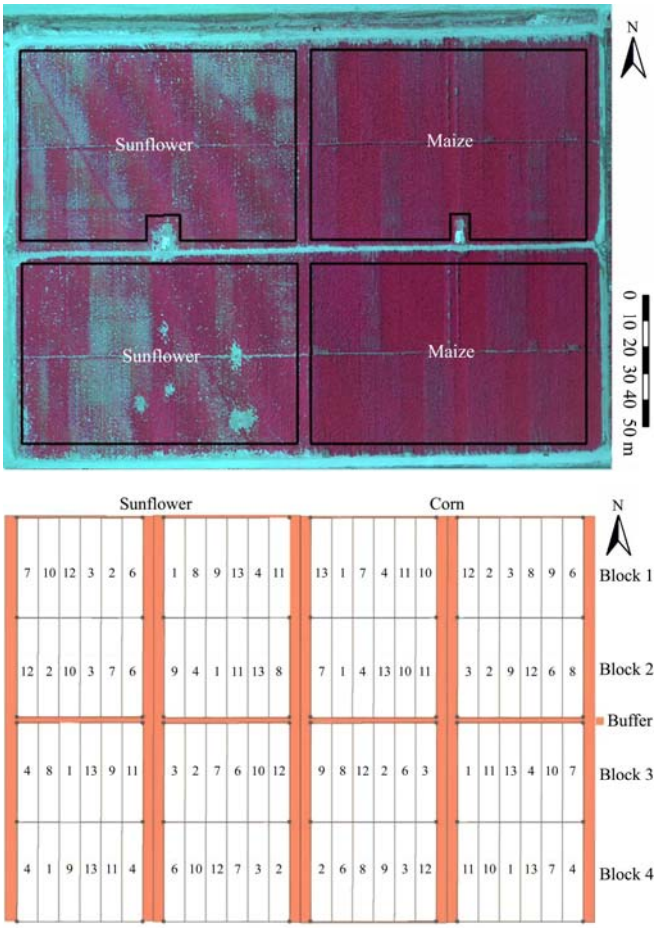

Figure 2 Airborne multispectral image taken on July 30, 2015 at the USDA-ARS Limited Irrigation Research Farm in Greeley, CO, USA (Top). The sunflower plots were in the western section and the maize plots were in the eastern section of the field. 12 Irrigation treatments: 1 = 100/100, 2 = 100/50, 3 = 80/80, 4 = 80/65, 6 = 80/40, 7 = 65/80, 8 = 65/65, 9 = 65/50, 10 = 65/40, 11 = 50/50, 12 = 40/40, 13 = 40/80. (Bottom)

2.3.2 Ground measurements

A neutron moisture meter (CPN-503 Hydroprobe, InstroTek, San Francisco, CA) was used to measure soil water content at the depths of 30 cm, 60 cm, 90 cm, and 120 cm in the middle row of each plot. Soil water content (SWC) at the 0-15 cm layer was measured by a portable time domain reflectometer (MiniTrace, Soilmoisture Equipment Corp, Santa Barbara, CA). The SWC measurement was taken twice to three times a week before and after irrigation; starting from the middle of the vegetative stage to the end of the crop growth season. Field capacity was estimated for each soil layer from SWC measurements obtained during the previous five years and current year. The SWC measured by neutron attenuation was assumed to represent the soil profile within 15 cm of the measurement depth. Because there was no evidence of water uptake from deeper soil layers, the observed SWD in each plot was calculated by summarizing soil water deficit from 0 to 1050 mm depth for maize and from 0 to 1350 mm for sunflower. More detailed information about soil water measurement and soil deficit calculation can be found in DeJonge et al.[15]

2.3.3 Remotely-sensed data

The Utah State University (USU) airborne digital remote sensing system[23,24] was used to acquire two airborne multispectral images over the research area, around solar noon on July 30 (DOY 211) (Figure 1) and September 10 (DOY 253) 2015. The imaging system consisted of three Kodak Megaplus digital frame cameras with interference filters centered in the spectral regions of green (0.545-0.560 m), red (0.665-0.680 m) and near infrared (0.795-0.809 m). Another camera included in the system was an Inframetrics 760 thermal-infrared scanner (8-12 m) to gain surface radiometric temperature over the field. The spatial resolutions of the multispectral bands and thermal band were about 0.3 m and 1.0 m, respectively. The white spots in the south side of the sunflower field indicated lack of stands because of planting skips (Figure 2). The pixels were excluded from analysis. Surface reflectance registered in the Red and NIR bands, form the airborne images, were used to determine OSAVI in Equation 10 (L = 0.16)[25]:

$$OSAVI = \frac{(1-L)(NIR-RED)}{NIR+RED+L} \quad (10)$$

Then LAI was determined from OSAVI in Equation (11)[26]:

$$LAI = (4 \times OSAVI - 0.8) \times (1 + 4.73 \times 10^{-6} \times e^{15.64 \times OSAVI}) \quad (11)$$

Then fractional canopy ground cover was determined from LAI by Equation (12)[27]:

$$f_c = 1 - \exp(-0.5LAI) \quad (12)$$

The k_{cb_mid}, $k_{cb\_ini,}$ and k_{cb_end} were obtained from the FAO-56 manual ($k_{cb\_ini,} = k_{cb\_end}$), and k_{cb_mid} was adjusted based on local climate (wind speed, relative humility and crop height)[17]. The length of each crop period (initial period, developing period, mid-period and end period) were also used as suggested in the FAO-56 procedure[17]. The k_{cb_mid} value at the airborne imagery acquisition day was adjusted by fractional canopy cover (f_c) derived from multispectral image. When f_c from multispectral image was greater than 0.8, $k_{cb,i}$ was equal to k_{cb_mid}; when f_c was smaller than 0.2, $k_{cb,i}$ was equal to $k_{cb\_ini,} = k_{cb\_end}$; and when f_c ranged from 0.2 to 0.8, $k_{cb,i}$ was linearly increased from k_{cb_ini} to k_{cb_mid}[17].

Crop water stress index was calculated for each image using Equations (1)-(3) and the baseline coefficients of maize were $T_c - T_a = -1.97VPD + 2.34$ and the baseline coefficients of sunflower were $T_c - T_a = -2.40VPD + 3.87$. CWSI values from pixels of each plot were extracted and averaged to represent CWSI for the plot.

2.4 Evaluation of optimized TAWr

To evaluate the performance of the optimized TAWr method on the soil water deficit prediction, the soil water balance model with the optimized TAWr (Model-TAWr) was compared with the observed soil water deficit. In addition, for comparison purpose, another simulation scenario was used to run the water balance model using empirical parameters, 7, 68, 20.25, and 120 mm for t_1, t_x, TAW_{min}, TAW_{max}, respectively (Model-FAO). These parameters were set based on soil texture, the rooting depth and crop growth stage measurements. Root Mean Square Error (RMSE), Nash-Sutcliffe coefficient (Nash), and Mean Absolute Error (MAE) were used to evaluate the goodness of model simulation[28,29].

3 Results and discussion

3.1 Crop water stress index

CWSI maps calculated from thermal imagery acquired on July 30 and September 10, 2015 are shown in Figure 3. On July 30, maize plants were in the late vegetative growth stage and under deficit irrigation. For example, the 40/40 and 40/80 treatments were irrigated only 40% of maximum ET water demand during that period. During this period, the accumulated water stress was very high (high CWSI values). Variations of CWSI within other treatment plots were not as obvious as those for treatments 40/40 and 40/80. The variation of CWSI may have been caused by the irrigation applied on July 29. Soil surface was partially wet when the image was taken. Maize plants on Sept 10 were about two weeks under deficit irrigation treatment in the maturation stage; thus, CWSI increased. Averaged CWSI values for each treatment are shown in Table 2. For maize plants on Jul 30, CWSI responded to deficit water treatment. CWSI value increased as irrigation amount decreased. When the crop reached the maturation stage the CWSI values increased, especially in those treatments that had deficit irrigation treatment applied in both late vegetative and maturation stages. That result (pattern) indicated that CWSI values indeed can reflect cumulated water stress during that crop growth stage. Treatment 40/80 depicted smaller CWSI values than those found for treatment 40/40, due to less water stress in the maturation stage.

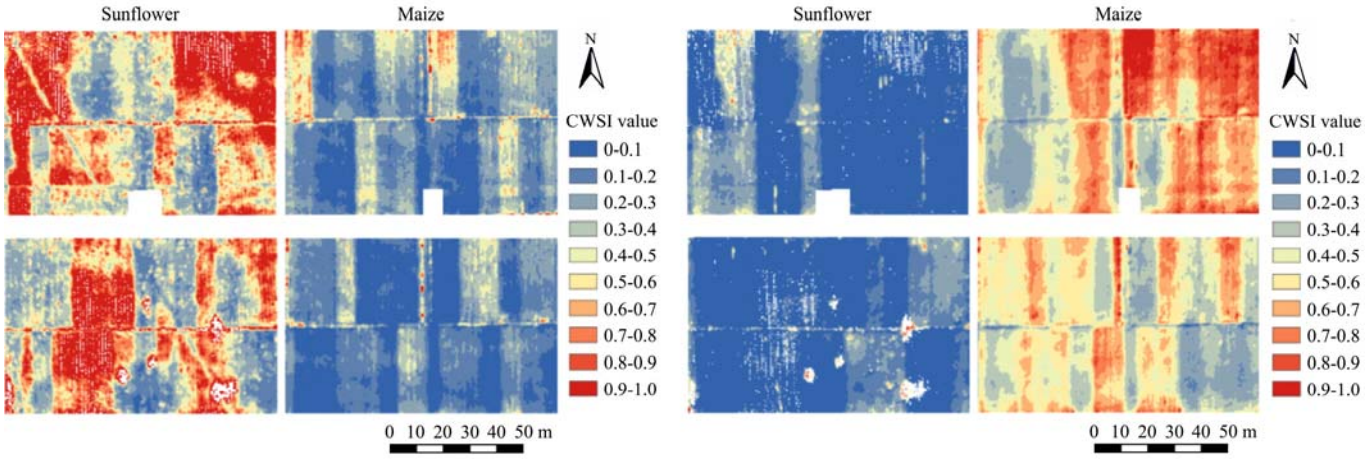

Figure 3 CWSI maps of study field on July 30 (Left) and September 10, 2015 (Right)

Table 2 Average CWSI for each treatment for maize and sunflower on July 30 and September 10, 2015

Treatment	Maize		Sunflower	
	Jul 30	Sept 10	Jul 30	Sept 10
100/100	0.07	0.26	0.33	0.02
100/50	0.07	0.51	0.28	0.24
80/80	0.10	0.43	0.39	0.14
80/65	0.09	0.42	0.49	0.18
80/40	0.14	0.63	0.39	**0.41**
65/80	0.18	0.33	0.69	0.14
65/65	0.22	0.61	0.62	0.24
65/50	0.23	0.66	0.78	0.23
65/40	0.20	0.66	0.68	**0.39**
50/50	0.25	0.67	0.82	0.26
40/40	0.40	0.74	0.82	**0.48**
40/80	0.39	0.41	0.86	0.25

Sunflower was planted about two weeks later than maize and canopy cover was relatively low on Jul 30 and water stress was shown clearly in the CWSI map. Average CWSI values for each treatment (Table 2) responded to water treatments with an average CWSI value of 0.31 for the 100% irrigation treatment, 0.42 for 80% the treatment, 0.69 for the 65% treatment, and 0.83 for the 50% and lower treatments. Deficit irrigation was only applied in the late vegetative and maturation stages. All the sunflower plants received full irrigation and were taken out of water stress in the reproductive stage (Aug 13 to Sept 2). By Sept 10, only the treatments with 40% showed some level of stress (CWSI > 0.39).

The relationship between CWSI and soil water deficit, estimated based on soil water content measurements, are given in Figure 4. CWSI increased with increasing soil water deficit. Although, a larger scatter of data points was observed for sunflower, for both crops, linear

regression relationships suggest that crop water stress calculated from canopy temperature could indicate soil water deficit in the root zone.

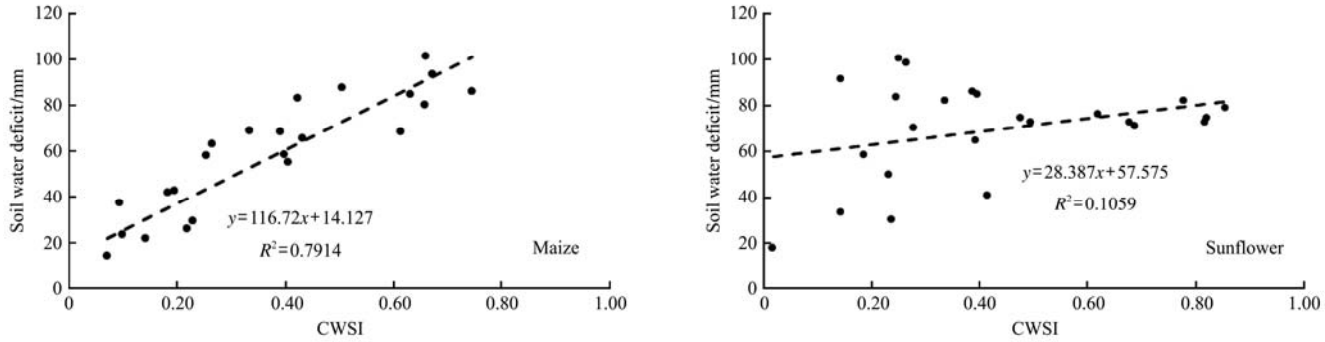

Figure 4 CWSI of each treatment on two image days plotted against soil water deficit in maize (Left) and sunflower (Right) root zone

3.2 Basal crop coefficient k_{cb}

The k_{cb} maps calculated from multispectral imagery acquired on Jul 30 and Sept 10, 2015 are shown in Figure 5. The k_{cb} values in all maize treatments reached its maximum value, 1.2, on Jul 30, except for 40/40 and 40/80 (k_{cb} = 1.03). The k_{cb} value for sunflower did not reach its maximum on Jul 30 (43 days after planting). The k_{cb} from treatment 100/100 sunflower was 0.96; which was significantly larger than those in 40/40 and 40/80 (k_{cb} = 0.70 and 0.74, respectively). On Sept 10, maize already had reached the maturation period, and deficit irrigated plots were resumed on Aug 24. A significant difference on k_{cb} values between deficit irrigation treatments was observed. For example, k_{cb} from the 100/100 treatment was 0.88, significantly higher than k_{cb} from 40/40 treatment (0.54). One could also notice that k_{cb} from 40/80 treatment (0.73) was also higher than that the corresponding k_{cb} value from 40/40, due to a larger water application in 40/80 treatment in the maturation stage. However, there was no significant k_{cb} difference among treatments for sunflower on Sept 10 due to the short period of resumed deficit irrigation. Deficit irrigation in sunflower plots was resumed on Sept 3, thus deficit irrigation had not impacted k_{cb} by Sept 10. However, we could still observe that treatment 40/40 had lower k_{cb} (0.7) than 100/100 and 40/80 treatment (0.81 and 0.75, respectively). Thus, k_{cb} derived from airborne multispectral imagery could reasonably describe the k_{cb} development under deficit irrigation for both crops. This result is consistent with the conclusion reached in previous researches[30-35].

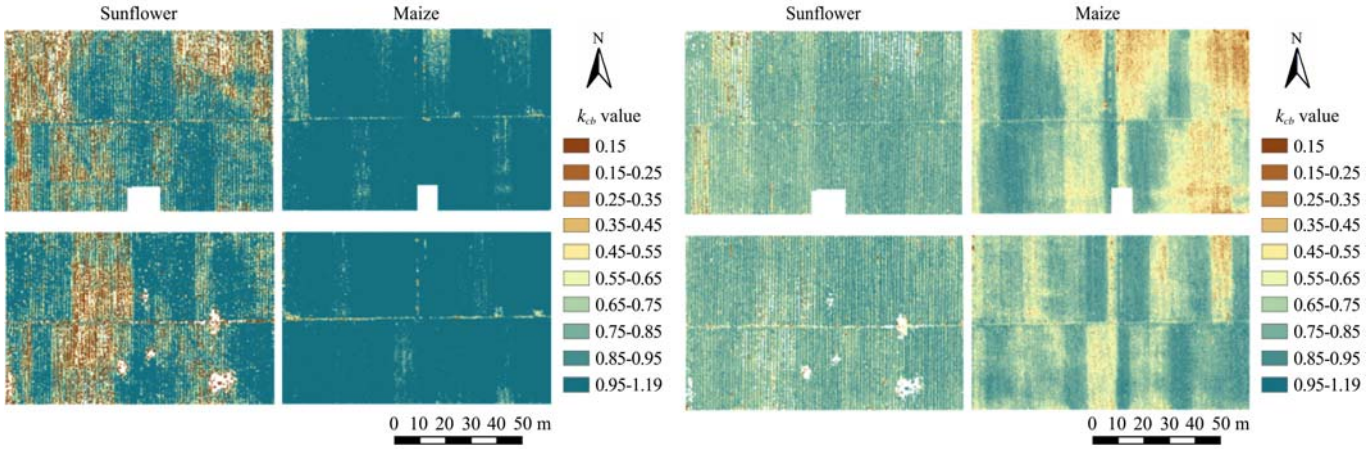

Figure 5 Crop coefficient (k_{cb}) maps of maize and sunflower on July 30 (Left) and September 10, 2015 (Right)

3.3 Estimated vs. measured soil water deficit

The optimal values of TAW_{max} are shown in Table 3. The proposed approach, using CWSI to optimize the soil water balance model, seems to produce reasonable values for the TAW_{max}. The average value of field capacity in this experimental field was 0.20-0.24 m^3/m^3. The root length distribution in the field varied considerably among treatments, where plants under deficit irrigation

treatments showed deeper root systems than fully watered plants[18]. Comas et al.[18] has found that maximum rooting depth for maize varied in 800-1050 mm in 2012. It is common to assume that soil volumetric water content at wilting point is 50% of field capacity[1]. Thus, the estimated TAW_{max} from the experimental data ranged in 80-126 mm. As shown in Table 3, the optimized TAW_{max} values for maize ranged from 71.5 mm for the 65/65 treatment to 136 mm for the full irrigation treatment. Sunflower has a generally deeper root system than maize and redistributes an even greater percentage of its roots to deeper soil depths[18]. Root depth has been found to range from 0.8 m to 1.5 m (FAO-56). The optimized TAW_{max} values for sunflower were much higher than those in maize. We also observed that the lowest optimized TAW_{max} values for both maize and sunflower were in treatments 65/65 and 65/50.

Table 3 Optimized TAW_{max} using airborne thermal derived CWSI for each treatment in maize and sunflower

Treatment	Maize	Sunflower
100/100	136.33	159.95
100/50	82.90	159.43
80/80	93.41	159.38
65/80	101.10	159.85
65/65	71.53	132.24
65/50	73.47	128.06
65/40	106.70	159.95
50/50	94.87	155.42
40/40	87.43	152.37
40/80	90.21	159.69

The optimized model (Model-TAW) resulted in an improved estimation of soil water deficit compare to the FAO-56 soil water balance model (SWB Model). Table 4 details the statistical analysis of the comparison between the two SWB models. By using TAW_{max} estimated from CWSI, the averaged Nash coefficient for all maize treatments increased from 0.17 to 0.72 and increased from 0.56 to 0.74 for sunflower. The average RMSE and MAE for all maize treatments decreased from 18.8 mm to 11.2 mm and from 15.4 mm to 8.6 mm, respectively, which reduced the RMSE and MAE by 40% and 44% compared to the original SWB model. Same as maize, the average RMSE and MAE for all sunflower treatments decreased from 14.6 mm to 11.3 mm and from 12.4 mm to 9.6 mm, respectively, which reduced both RMSE and MAE by 22% compared to the SWB model. Figure 6 plots the predicted soil water deficit by the optimized model and SWB model versus measured soil water deficit for treatments 100/100, 65/65, and 40/80, for instance. In the fully watered treatment, the two models performed similarly. Soil water deficit was maintained less than 60 mm for fully watered maize and about 80 mm for fully watered sunflower throughout the growing season. The optimization procedure may not give an optimized TAW_{max} value for well-watered plots since the CWSI would be close to zero and the change of TAW_{max} would not substantially influence crop transpiration. Both models showed the trend of increasing soil water deficit in the late vegetative stage, decreasing soil water deficit in the reproductive stage when full irrigation was applied, and increasing again towards the late season. However, the optimized model using CWSI better responded to soil water deficit observation in treatment 65/65 and 40/80 than the SWB model, especially in the maturation stage, where the SWB model underestimated the measured soil water deficit.

Table 4 Statistical analysis of modeled and observed soil water deficit (mm) by Model-TAW: soil water balance model with optimized TAW; and Model-FAO: soil water balance model with experienced TAW

Crop	Treatment	Optimized model			Soil water balance model		
		Nash	RMSD	MAE	Nash	RMSD	MAE
Maize	100/100	0.27	15.22	12.03	0.20	15.89	12.40
	100/50	0.87	10.85	8.45	0.74	15.04	12.24
	80/80	0.66	10.98	8.40	0.55	12.71	10.56
	65/80	0.69	12.49	9.83	0.60	14.14	10.98
	65/65	0.51	13.39	10.38	-1.82	32.24	25.61
	65/50	0.80	10.02	7.64	-0.44	26.65	22.12
	65/40	0.89	10.09	7.99	0.84	12.07	10.29
	50/50	0.86	9.69	7.32	0.55	17.23	14.65
	40/40	0.86	9.08	6.81	0.17	22.37	19.23
	40/80	0.78	10.51	7.54	0.26	19.39	16.04
Sunflower	100/100	0.32	17.66	15.49	0.09	20.36	18.14
	100/50	0.88	11.15	9.02	0.78	15.31	12.98
	80/80	0.69	11.67	10.31	0.42	15.98	13.00
	65/80	0.64	10.46	8.96	0.29	14.65	12.23
	65/65	0.75	9.91	8.16	0.73	10.32	8.13
	65/50	0.85	9.18	7.91	0.84	9.35	8.05
	65/40	0.85	11.94	9.50	0.73	16.00	13.16
	50/50	0.88	8.80	7.39	0.78	11.88	10.01
	40/40	0.86	11.12	9.32	0.76	14.19	12.27
	40/80	0.66	11.69	10.04	0.22	17.59	15.83

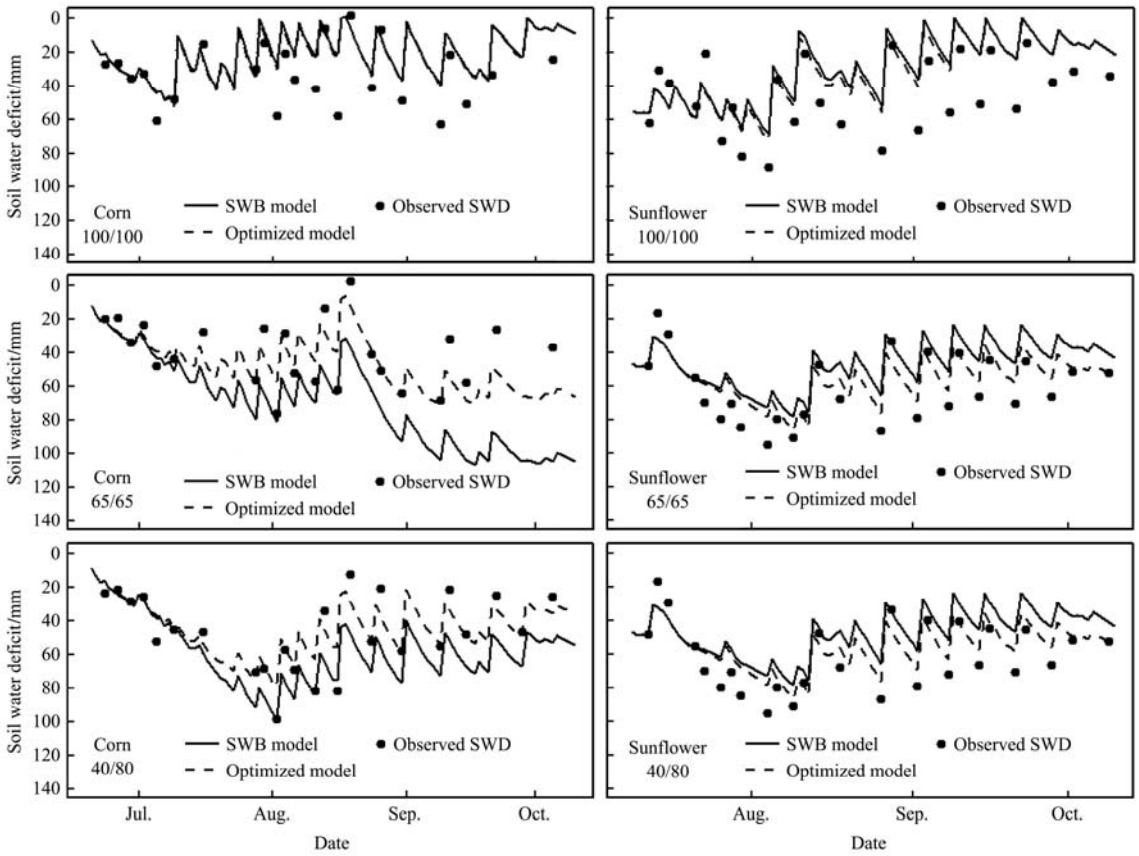

Figure 6 Comparison of the observations, the optimized daily soil water deficit with airborne imagery data by Model-TAW, and FAO-56 SWB model

4 Conclusions

In this study, crop water stress index derived from airborne thermal imagery was incorporated into a soil water balance model to determine the total available water in the root zone and to improve the estimate of actual soil water deficit. The *TAWr* was estimated by calibrating the soil water balance model using CWSI as an input. A general agreement was found between the estimated soil water deficit from the proposed approach with measured soil water deficit in the deficit irrigation experiment for maize and sunflower. The statistical analyses indicated that the *TAWr* estimated from CWSI significantly improved the estimation of soil water deficit values; which reduced the mean absolute error and root mean square error by 40% and 44% for maize and 22% for sunflower compared to the standard FAO-56 model. The proposed procedure works better for crops under deficit irrigation conditions. It is anticipated that the approach presented here can be further improved if more airborne multispectral images are available for integration in the optimization procedure.

[References]

[1] Allen R G, Pereira L S, Raes D, Smith M. Crop evapotranspiration-Guidelines for computing crop water requirements-FAO Irrigation and drainage paper 56. FAO, Rome. 1998; 300(9).

[2] Annandale J G, Campbell G S, Olivier F C, Jovanovic N Z. Predicting crop water uptake under full and deficit irrigation: An example using pea (Pisum sativum L. cv. Puget). Irrigation Science, 2000; 19(2): 65–72.

[3] Campos I, González-Piqueras J, Carrara A, Villodre J, Calera A. Estimation of total available water in the soil layer by integrating actual evapotranspiration data in a remote sensing-driven soil water balance. Journal of Hydrology, 2016; 534: 427–39.

[4] Steduto P, Hsiao T C, Raes D, Fereres E. AquaCrop—The FAO crop model to simulate yield response to water: I. Concepts and underlying principles. Agronomy Journal, 2009; 101(3): 426–37.

[5] Hsiao T C, Heng L, Steduto P, Rojas-Lara B, Raes D, Fereres E. AquaCrop—the FAO crop model to simulate yield response to water: III. Parameterization and testing for maize. Agronomy Journal, 2009; 101(3): 448–59.

[6] Sánchez N, Martínez-Fernández J, Calera A, Torres E, Pérez-Gutiérrez C. Combining remote sensing and in situ soil moisture data for the application and validation of a distributed water balance model (HIDROMORE). Agricultural Water Management, 2010; 98(1): 69–78.

[7] Neale C M U, Geli H M E, Kustas W P, Alfieri J G, Gowda P H, Evett S R, et al. Soil water content estimation using a remote sensing based hybrid evapotranspiration modeling approach. Advances in Water Resources, 2012; 50: 152–61.

[8] Campos I, Balbontín C, González-Piqueras J, González-Dugo M P, Neale C M U, Calera A. Combining a water balance model with evapotranspiration measurements to estimate total available soil water in irrigated and rainfed vineyards. Agricultural Water Management, 2016; 165: 141–52.

[9] Padhi J, Misra R K, Payero J O. Estimation of soil water deficit in an irrigated cotton field with infrared thermography. Field Crops Research, 2012; 126: 45–55.

[10] Li B, Wang T L, Sun J. Crop water stress index for off-season greenhouse green peppers in Liaoning, China. Int J Agric & Biol Eng, 2014; 7(3): 28–35

[11] Zia-Khan S, Du W Y, Spreer W, Spohrer K, He X K, Müller J. Assessing crop water stress of winter wheat by thermography under different irrigation regimes in North China Plain. Int J Agric & Biol Eng, 2012; 5(3): 24–34.

[12] Zia-Khan S, Spohrer K, Du W Y, Spreer W, Romano G, He X K, et al. Monitoring physiological responses to water stress in two maize varieties by infrared thermography. Int J Agric & Biol Eng, 2011; 4(3): 7–15.

[13] Idso S B, Jackson R D, Pinter P J, Reginato R J, Hatfield J L. Normalizing the stress-degree-day parameter for environmental variability. Agricultural Meteorology, 1981; 24: 45–55.

[14] Jackson R D, Idso S B, Reginato R J, Pinter P J. Canopy temperature as a crop water stress indicator. Water Resources Research, 1981; 17(4): 1133–8.

[15] DeJonge K C, Taghvaeian S, Trout T J, Comas L H. Comparison of canopy temperature-based water stress indices for maize. Agricultural Water Management, 2015; 156: 51–62.

[16] Taghvaeian S, Comas L, DeJonge K C, Trout T J. Conventional and simplified canopy temperature indices predict water stress in sunflower. Agricultural Water Management, 2014; 144:69–80.

[17] Allen R G, Pereira L S, Raes D, Smith M. Crop evapotranspiration-Guidelines for computing crop water requirements-FAO Irrigation and drainage paper 56. FAO, Rome, 1998; 300(9): D05109.

[18] Comas L H, Becker S R, Cruz V M, Byrne P F, Dierig D A. Root traits contributing to plant productivity under drought. Frontiers in plant science, 2013; 4:442.

[19] Colaizzi P D, Barnes E M, Clarke T R, Choi C Y, Waller P M. Estimating soil moisture under low frequency surface irrigation using crop water stress index. Journal of Irrigation and Drainage Engineering, 2003; 129(1): 27–35.

[20] Jensen M E, Robb D C, Franzoy C E. Scheduling irrigations using climate-crop-soil data. Proceedings of the American Society of Civil Engineers, Journal of the Irrigation and Drainage Division, 1970; 96(IRI): 25–38.

[21] Trout T J, DeJonge K C. Water Productivity of Maize in the U.S. High Plains. Irrigation Science, 2017; 1–16.

[22] Mersmann O, Trautmann H, Steuer D, Bischl B, Deb K. Package "mco": Multiple Criteria Optimization Algorithms and Related Functions. URL: https://cran.r-project.org/web/packages/mco/mco.pdf: 2014.

[23] Neale C M U, Crowther B G. An airborne multispectral video/radiometer remote sensing system: Development and calibration. Remote Sensing of Environment, 1994; 49(3): 187–94.

[24] Cai B, Neale C M U. A method for constructing three dimensional models from airborne imagery. 17th Biennial Workshop on Color Photography and Videography in Resource Assessment, Reno, NV 1999.

[25] Rondeaux G, Steven M, Baret F. Optimization of soil-adjusted vegetation indices. Remote sensing of environment, 1996; 55(2): 95–107.

[26] Anderson M, Neale C, Li F, Norman J, Kustas W, Jayanthi H, et al. Upscaling ground observations of vegetation water content, canopy height, and leaf area index during SMEX02 using aircraft and Landsat imagery. Remote sensing of environment, 2004; 92(4): 447–64.

[27] Kustas W P, Norman J M. Evaluation of soil and vegetation heat flux predictions using a simple two-source model with radiometric temperatures for partial canopy cover. Agricultural and Forest Meteorology, 1999; 94(1): 13–29.

[28] Nash J E, Sutcliffe J V. River flow forecasting through conceptual models part I—A discussion of principles. Journal of hydrology, 1970; 10(3): 282–90.

[29] Willmott C J. Some comments on the evaluation of model performance. Bulletin of the American Meteorological Society, 1982; 63(11): 1309–13.

[30] Hunsaker D J, Pinter P J, Barnes E M, Kimball B A. Estimating cotton evapotranspiration crop coefficients with a multispectral vegetation index. Irrigation Science, 2003; 22(2): 95–104.

[31] Hunsaker D J, Pinter P J, Kimball B A. Wheat basal crop coefficients determined by normalized difference vegetation index. Irrigation Science, 2005; 24(1): 1–14.

[32] Allen R G, Pereira L S. Estimating crop coefficients from fraction of ground cover and height. Irrigation Science, 2009; 28(1): 17–34.

[33] Trout T J, Johnson L F, Gartung J. Remote sensing of canopy cover in horticultural crops. HortScience, 2008; 43(2): 333–7.

[34] Bryla D R, Trout T J, Ayars JE. Weighing lysimeters for developing crop coefficients and efficient irrigation practices for vegetable crops. HortScience, 2010; 45(11): 1597–604.

[35] Neale C M, Bausch W C, Heermann D F. Development of reflectance-based crop coefficients for corn. Transactions of the ASAE, 1990; 32(6): 1891–900.